

FreeCable™ four-component analysis: An interpretation workflow of real data in complex marine and subsurface environment

Introduction

The principle of the FreeCable acquisition method is to operate Midwater Stationary Cables (MSCs) controlled individually by a pair of unmanned surface vehicles named Recording Autonomous Vessels (RAVs), each MSC being equipped by four-component seismic sensors and tied at both extremities to a RAV. This new acquisition system demonstrated the value of recording full-azimuth, full-offset, high-fold, broadband and four-component data through extensive tests, a pilot survey (Haumonté and Manin, 2017), flexible survey designs to tackle the subsurface imaging and reservoir characterization challenges, and measurement quality of the inline geophone.

To exploit multi-component data further in a complicated subsurface geology due to the presence of salt and a complex marine environment (large variations in water depth, irregular seabed), a polarization analysis estimating the direction of wave propagation and the direction of particle motion was performed, based on finite-difference 2D elastic modelling. The 2D model used in the study represents a rough seabed with flat reflectors underneath (Figure 1).

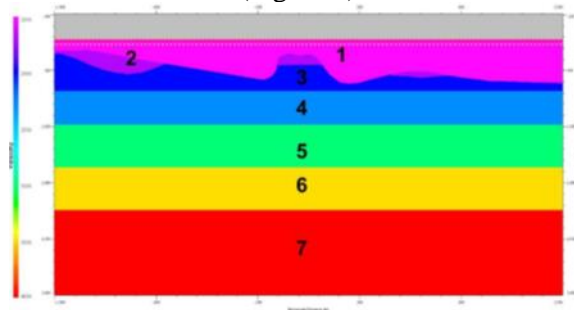


Figure 1: 2D model (Manin and Haumonté, 2018).

The direction of particle motion is estimated by computing the angle between the vertical geophone and the inline geophone. Figure 2 displays two shot gathers overlaid by a colour code representing this angle. The adopted convention is such that blue corresponds to 0 degrees (horizontal, from left to right), green to 90 degrees (vertical), and red to 180 degrees (horizontal, from right to left). This representation enables to directly interpret the seismic events:

- The strong direct arrivals (straight lines) can be seen as travelling left and right from the shots
- The reflections on the flat layers (hyperbolae) propagate almost vertically with a motion angle close to vertical (see blue arrow)
- The directly reflected waves on slanted cliffs (hyperbolae close to straight lines) propagate with an angle close to horizontal, confirmed by the motion angle and a propagation direction opposed to the direct arrival (see black arrow on Figure 2)
- It can also be remarked that wave propagation direction and particle motion direction are equivalent, which is coherent with the fact that only P-waves are recorded in the water.

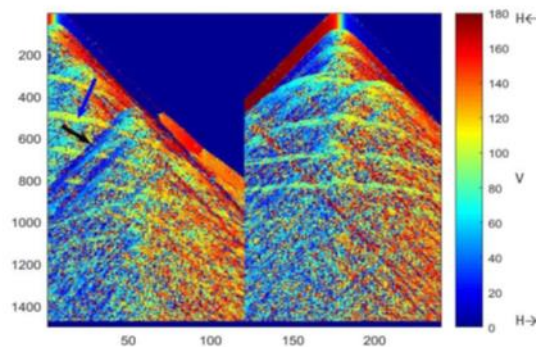


Figure 2: Polarization angle of two shot gathers for MSCs (Manin and Haumonté, 2018).

Theory

In this section, we address the following issues:

- Presentation of the equations used to perform the polarization analysis of the seismic data recorded during the pilot survey (for full details, see cited reference)
- Description of the workflow and results of the four-component analysis on 3D receiver gather.

The signal is tied to the four-component station in a single point of measurement by the following equations:

$$\begin{aligned}
 H &= \rho c * (S(t) - S(t - \tau(nz))) \\
 X &= nx * (S(t) - S(t - \tau(nz))) \\
 Y &= ny * (S(t) - S(t - \tau(nz))) \\
 Z &= nz * (S(t) + S(t - \tau(nz)))
 \end{aligned}$$

Where H is the hydrophone, X is the inline geophone, Y is the crossline geophone and Z the vertical geophone. S is the incident upgoing signal with a unit vector of propagation of (nx ,ny ,nz) components and $nx^2 + ny^2 + nz^2 = 1$. Because P-waves are only present in water, this unit vector is also the unit vector of the particle velocity. By construction, nx is in the direction parallel to the MSC and ny in the direction perpendicular to the MSC.

The delayed term of τ is the ghost signal. τ delay is function of nz. With p the MSC depth and c the sound velocity in water,

$$\tau = nz * \frac{2p}{c}$$

At vertical incidence where nz equals 1 and nx and ny equal 0, we get the usual two-way travel-time expression. The unknowns of the above equation system are: S the deghosted signal, and nx, ny and nz knowing that if two of them are known, the third is calculated by the norm. The water impedance ρc is not considered as an unknown and the knowns are H, X, Y and Z data recorded in a small temporal window including the seismic arrival which is analyzed. The observation of the equation system yields two interesting results:

- X/H and Y/H cancel the ghosted signal it has in common and yield straightly nx and ny
- Z is the sole measurement with a positive ghost; for deghosting by summation, H and Z can be combined but nz needs to be known.

Method

Here, we focus on the analysis of the direct arrivals. This arrival type is quasi-horizontal which means that nz is small. In addition, the position of the shot and the receiver yield the azimuth i.e., the angle between the source-receiver vector and the MSC vector in a very accurate way (Figure 3). Therefore, the constants entering in the calculation of nx and ny can be calibrated under the form $nx=\cos(\text{azimuth})$ and $ny=\sin(\text{azimuth})$.

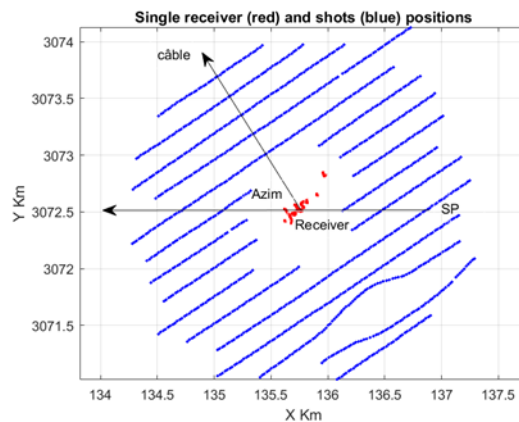


Figure 3: Geometry analysis (3D receiver gather).

For performing this analysis, it is important that the same pre-processing is applied to each sensor i.e., sensitivity correction specific for each sensor type, value of water impedance (25.117 in our unit system)

and 15Hz low-cut filter. It is assumed that the wave direction hence the n_x and n_y coefficients are not frequency-dependent and the signal-to-noise ratio is optimum in the selected time window. Figure 4 represents the regression of Y and H and its best fit versus the shot point azimuth in a 200ms window centered around the direct arrival. It can be observed that the fit to a theoretical sinusoid (and after the impedance value is set to 22) is excellent. Figure 5 shows the value of n_y (Y/H) vs YH and proves this formulation is universal. It enables to calculate n_y at each receiver point using the Y and H regression.

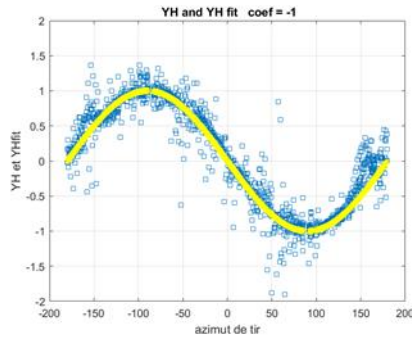


Figure 4: Y and H regression vs shot point azimuth.

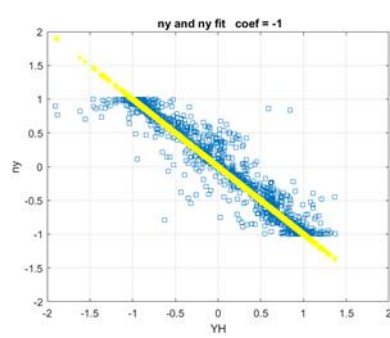


Figure 5: n_y vs Y and H regression.

In the case of the X component, the analysis results are less satisfactory, at least for the first arrival which is studied here (Figure 6 and Figure 7). Except for the term in cosine instead of sine, the geophone sensor having the same sensitivity and with the same water impedance, the cluster of points should match with the cosine curve with the same fit coefficient.

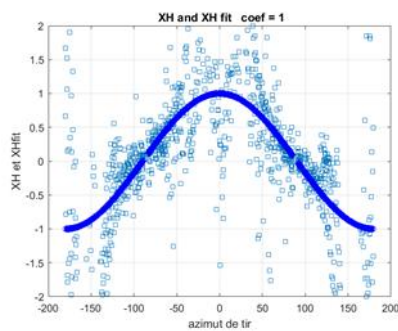


Figure 6: X and H regression vs shot point azimuth.

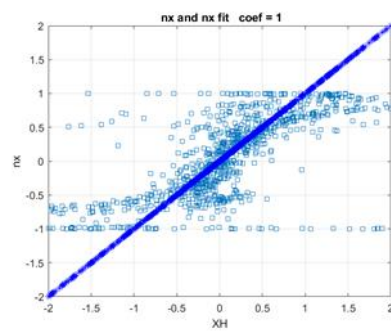


Figure 7: n_x vs X and H regression.

Examples

Now, these formulation and calibration can be applied to a four-component receiver gather (#142). Figure 8 and 9 show the H, X, Y and Z component, respectively.

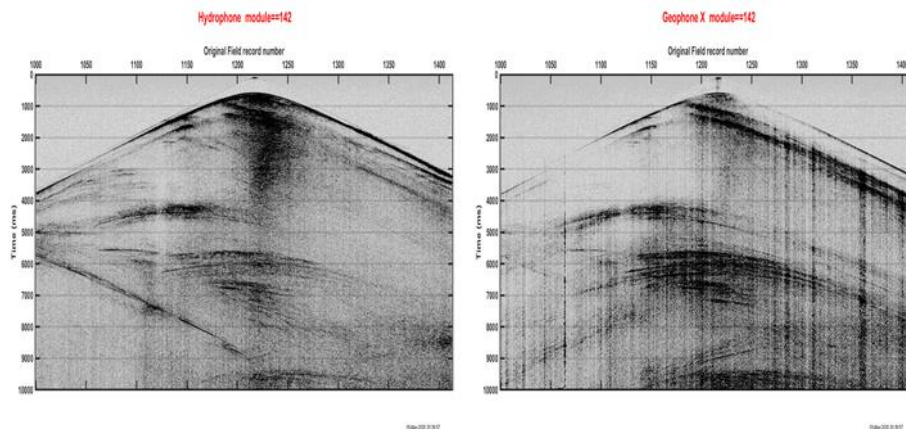


Figure 8: H component (left) and X component (right) of the #142 receiver gather.

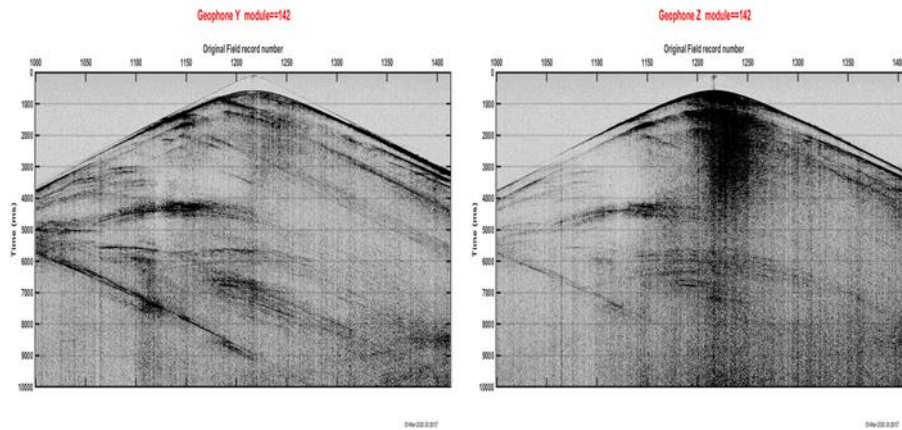


Figure 9: Y component (left) and Z component (right) of the #142 receiver gather.

To compute n_y (Figure 10) and n_x (Figure 11) using the formulae already mentioned, the correlation is done in a sliding window (which moves from one sample each time) between H and Y and H and X. The length of the correlation window is 42ms.

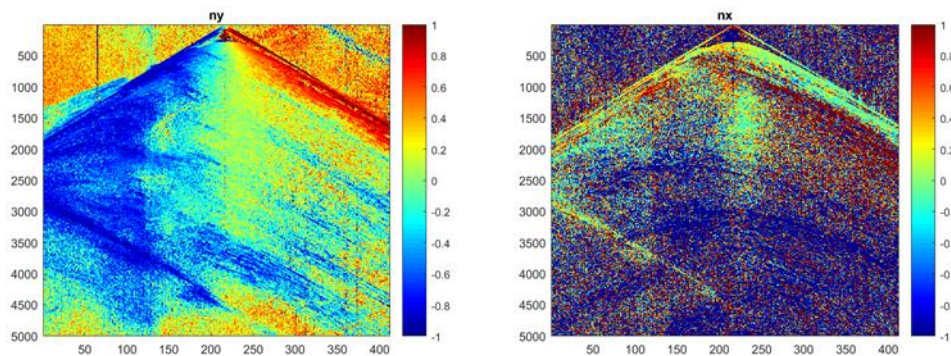


Figure 10: n_y map of the propagation unit vector. Figure 11: n_x map of the propagation unit vector.

It can be observed on those two latest figures that the wave direct arrival is compliant with what can be expected: n_y equals -1 or 1 and n_x equals 0. The very visible diffraction initiated at 3s twt on the left of the figures has a n_y value close to -1 and a n_x value close to 0. From an interpretation perspective, this is a quasi-horizontal wave which is generated by a surface diffractor, most probably a cliff on the seafloor. Another interpretation example is the steep-dipping arrival at the left in the 3.9-4.9s and shot point #1095-1175 window (see Figure 8). This seismic event differentiates from other surrounding events by its direction i.e., n_y close to 1 and n_x equals 0, the other events having a strong n_x value.

Conclusions

The results obtained with real acquisition data are remarkably in line with the modelling analysis. The single-station, four-component theoretical considerations, workflow, and results presented in this paper demonstrate that the FreeCable technology and method enable to record, process and interpret qualitatively seismic data in a complex marine and subsurface environment. For example, it was shown that the analysis of the propagation direction of a diffracted wave allows to interpret its generator to be a seafloor irregularity. This technique is independent of any spatial sampling requirements. Those remarkable results using the crossline-geophone measurement (Y) and the inline-geophone measurement (X) of the MSCs open new ways for performing high-quality, high-fidelity (4C) interpretation of marine seismic data.

References

Haumonté, L. and Manin, M. [2017]. A paradigm shift in marine seismic: Broadband full-offset full-azimuth 4-C acquisition with midwater stationary cable. 87th Annual International Meeting, SEG, Expanded Abstracts.